Bioorganic & Medicinal Chemistry 17 (2009) 2902–2912

Contents lists available at ScienceDirect

Bioorganic & Medicinal Chemistry

journal homepage: www.elsevier.com/locate/bmc

Sesquiterpene-like inhibitors of a 9-*cis*-epoxycarotenoid dioxygenase regulating abscisic acid biosynthesis in higher plants

Jason Boyd, Yuanzhu Gai, Ken M. Nelson, Erica Lukiwski, James Talbot [†], Mary K. Loewen, Stacey Owen, L. Irina Zaharia, Adrian J. Cutler, Suzanne R. Abrams [*,‡], Michele C. Loewen [‡]

Plant Biotechnology Institute, National Research Council of Canada, 110 Gymnasium Place, Saskatoon, SK, Canada S7N 0W9

ARTICLE INFO

Article history:
Received 21 December 2008
Revised 30 January 2009
Accepted 31 January 2009
Available online 8 February 2009

Keywords:
Abscisic acid biosynthesis
ABA biosynthesis inhibitor
9-*cis*-Epoxycarotenoid dioxygenase
Carotenoid metabolism
Xanthoxin analog
ABA analog

ABSTRACT

Abscisic acid (ABA) is a carotenoid-derived plant hormone known to regulate critical functions in growth, development and responses to environmental stress. The key enzyme which carries out the first committed step in ABA biosynthesis is the carotenoid cleavage 9-*cis*-epoxycarotenoid dioxygenase (NCED). We have developed a series of sulfur and nitrogen-containing compounds as potential ABA biosynthesis inhibitors of the NCED, based on modification of the sesquiterpenoid segment of the 9-*cis*-xanthophyll substrates and product. In in vitro assays, three sesquiterpene-like carotenoid cleavage dioxygenase (SLCCD) inhibitor compounds **13**, **17** and **18** were found to act as inhibitors of *Arabidopsis thaliana* NCED 3 (AtNCED3) with K_i's of 93, 57 and 87 μM, respectively. Computational docking to a model of AtNCED3 supports a mechanism of inhibition through coordination of the heteroatom with the non-heme iron in the enzyme active site. In pilot studies, pretreatment of osmotically stressed *Arabidopsis* plants with compound **13** resulted lower levels of ABA and catabolite accumulation compared to levels in mannitol-stressed plant controls. This same inhibitor moderated known ABA-induced gene regulation effects and was only weakly active in inhibition of seed germination. Interestingly, all three inhibitors led to moderation of the stress-induced transcription of AtNCED3 itself, which could further contribute to lowering ABA biosynthesis *in planta*. Overall, these sesquiterpenoid-like inhibitors present new tools for controlling and investigating ABA biosynthesis and regulation.

1. Introduction

Abscisic acid (**1**, ABA) is a plant hormone involved in the regulation of important developmental functions including seed maturation, desiccation tolerance and dormancy, as well as adaptation to environmental stress through stomatal closure and modification of gene expression.[1–3] The biosynthesis of ABA **1** begins with isopentenyl diphosphate which enters the mevalonic acid-independent 2-C-methyl-D-erythritol-4-phosphate pathway producing plastidic isoprenoids, including carotenoids.[4] Enzymatic cleavage of C_{40}-carotenoid *cis*-xanthophylls (neoxanthin **2** and violaxanthin **3**) at the 11′–12′ double bond by a 9-*cis*-epoxycarotenoid dioxygenase (NCED) produces C_{15} (xanthoxin **4**) and C_{25} metabolites and represents the first committed step in ABA biosynthesis (Fig. 1). Xanthoxin **4** is subsequently converted by an alcohol dehydrogenase (ABA2) into abscisyl aldehyde **5**, which is oxidized to ABA **1** by an abscisic aldehyde oxidase (AAO3).[3] The catabolism of ABA occurs principally through oxidation of one of the methyl groups of the ring (8′-carbon atom, using convention for ABA numbering) mediated by members of a class of P450 monooxygenase enzymes, CYP 707A.[5] The catabolite phaseic acid (**6**, PA) which occurs as the result of reversible cyclization of 8′-hydroxyABA, is reduced by an unknown reductase to afford dihydrophaseic acid (**7**, DPA). ABA can also be metabolized to the glucose conjugate **8**.[3]

First identified in maize (VP14), NCEDs have also been found in a variety of other species including *Arabidopsis thaliana* (AtNCED3), bean (PvNCED1), tomato (LeNCED1), avocado (PaNCED1 and PaNCED3) and cowpea (VuNCED1).[6–11] AtNCED3 is a member of the carotenoid cleavage enzyme family of *A. thaliana*, which consists of nine enzymes.[12] In general, the family is characterized by a plastid-targeting transit peptide, an amphipathic α-helix domain and a catalytic domain which contains four conserved histidine residues responsible for non-heme iron coordination. AtNCED3 is found in both the stroma and bound to the thylakoid membrane, accounts for NCED activity in roots, contributes to NCED activity in developing seeds and is the major stress-induced NCED in leaves of *A. thaliana*.[12] Recently, immunohistochemical analysis revealed that the AtNCED3 protein is detected exclusively in the vascular parenchyma cells of water-stressed plants.[13]

* Corresponding author. Tel.: +1 306 975 5569; fax: +1 306 975 4839.
E-mail address: sue.abrams@nrc-cnrc.gc.ca (S.R. Abrams).
† Current address: Department of Biochemistry, University of Saskatchewan, 107 Wiggins Road, Saskatoon, SK, Canada S7N 0W5.
‡ These authors contributed equally to this work.

0968-0896/$ - see front matter Crown Copyright © 2009 Published by Elsevier Ltd. All rights reserved.
doi:10.1016/j.bmc.2009.01.076

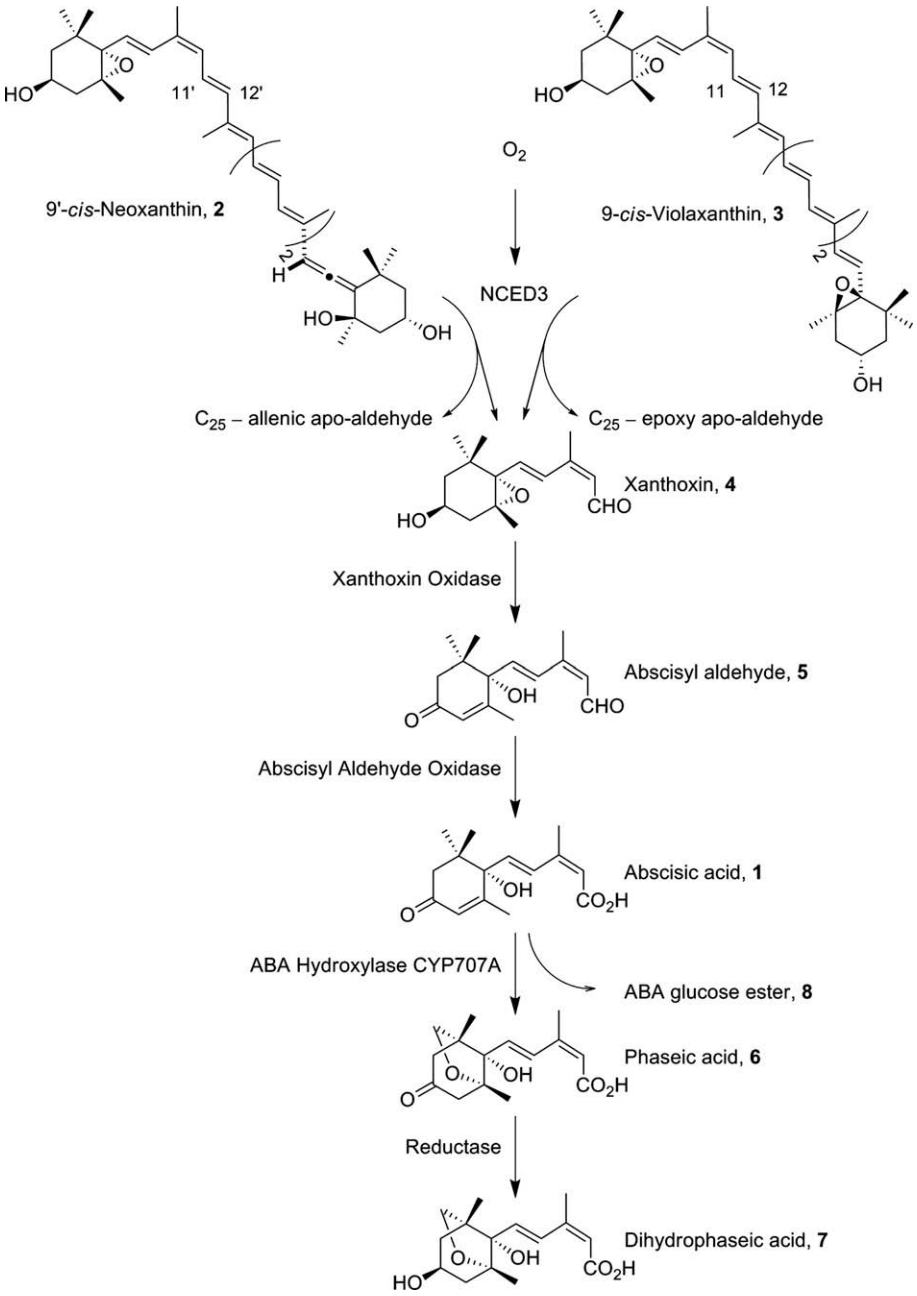

Figure 1. ABA biosynthesis and catabolism pathway of higher plants from the committed step of C_{40}-carotenoid cleavage of either 9-*cis*-neoxanthin **2** or 9-*cis*-violaxanthin **3** by AtNCED3.

Due to ABA's important role in plant physiology, significant effort has been expended on investigating functional aspects of ABA **1** biosynthesis, regulation and action. ABA-deficient mutants are powerful tools for elucidating ABA's role *in planta*, as are chemical inhibitors of ABA **1** biosynthesis which have broad applicability to many plant species. General carotenoid biosynthesis inhibitors such as fluridone, a potent broad spectrum herbicide that inhibit phytoene desaturase in the carotenoid biosynthesis pathway, have been used to inhibit ABA **1** biosynthesis.[14,15] While fluridone does inhibit ABA **1** biosynthesis, a corresponding general repression of the carotenoid biosynthesis pathway limits its application for biochemical investigations including those of carotenoid cleavage enzymes and products. To address this problem, Abamine compounds **9** and **10** were developed as inhibitors of NCED's, based on early observations that a number of inhibitors of soybean lipoxygenase were effective in reducing ABA accumulation in stressed soybean cell cultures and seedlings.[16] One of the active compounds, nordihydroguaiaretic acid, served as the starting structure for generation of analogs with improved NCED inhibitory activity, leading to development of the tertiary amines Abamine (**9**, ABM) and Abamine SG (**10**, ABM-SG) (Fig. 2).[17,18] *Arabidopsis* plants treated with ABM **9** showed a significant decrease in drought tolerance and under simulated osmotic stress ABM **9** inhibited stomatal closure in spinach leaves. The latter effect was counteracted by co-application of ABA **1**. ABM-SG **10** strongly inhibited the expression of ABA-responsive and catabolic genes in plants under osmotic stress. Finally, both ABM **9** and ABM-SG **10** reduced ABA metabolite accumulation by 35% and 77%, respectively and were shown to act as competitive inhibitors of the cowpea NCED enzyme, with K_i's of 18.5 μM and 38.8 μM, respectively.

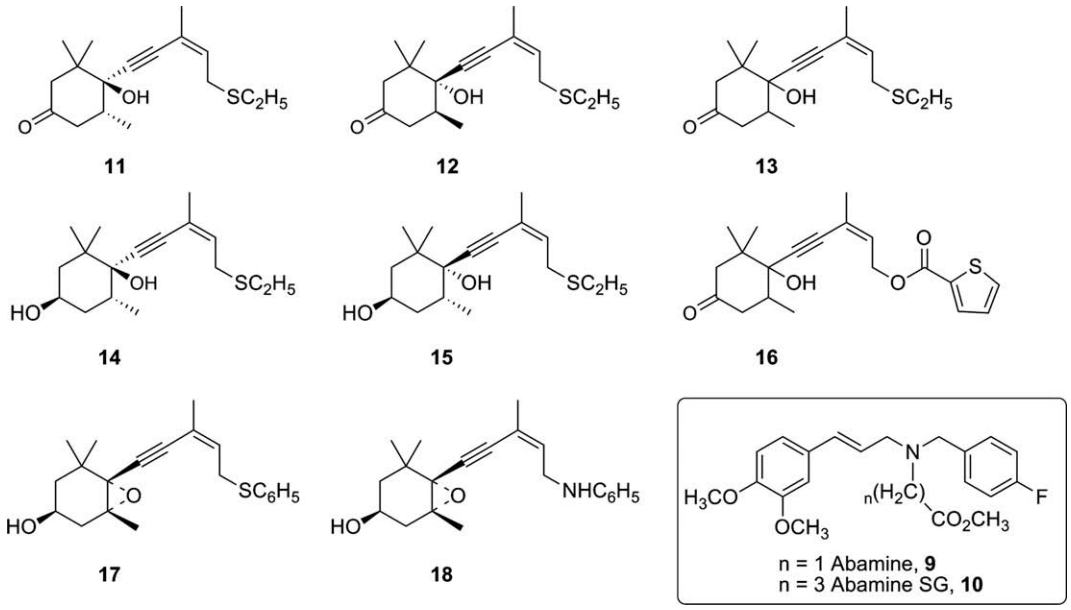

Figure 2. Structures of AtNCED3 SLCCD inhibitors.

In this report we describe the design, synthesis and characterization of a novel set of sesquiterpene-like carotenoid cleavage dioxygenase (SLCCD) inhibitors **11–18**. The current compounds were designed starting with the sesquiterpenoid subunit of the substrate and product of the NCED enzyme. Of eight initial inhibitors designed and tested (Fig. 2), three were found to inhibit recombinant AtNCED3 activity strongly. These have been fully characterized in vitro, with kinetic inhibition constants comparing favorably to those of the ABM-type compounds. Computational docking of the inhibitors correlated with these findings and supported the proposed functional mechanism. In preliminary in vitro analyses, one inhibitor in particular, SLCCD inhibitor compound **13** was found to moderate ABA-responsive genes and ABA metabolism. Interestingly, all three inhibitors reduced expression of AtNCED3, presenting a second mechanism for inhibition of ABA **1** biosynthesis by the molecules.

2. Results

2.1. Design and synthesis of the SLCCD inhibitors

The present compounds were designed to incorporate the 9-*cis* double bond geometry of the substrates and product of AtNCED3 as well as a heteroatom at carbon 12 (carotenoid numbering) of the inhibitor molecules. All of the SLCCD inhibitors **11–18** were synthesized from 4-oxoisophorone **19** (Fig. 3). Bakers′ yeast reduction of **19** afforded (−)-*(R)*-2,2,6-trimethylcyclohexa-1,4-dione[19] which was converted into chiral nonracemic allylic alcohols **20**, **21**, **23** and **24**.[20] Racemic allylic alcohol **22** was prepared in a similar manner, except that reduction of **19** was accomplished using zinc in acetic acid.[21] The terminal allylic alcohols were then converted to the corresponding ethyl sulfides by reaction with ethyl disulfide in the presence of tributylphosphine.[22] Inhibitor **16** was obtained by reacting 2-thiopheneacetyl chloride and allylic alcohol **22** (protected as the neopentylglycol ketal). The xanthoxin-like allylic alcohol **22** was prepared through a Sonogashira coupling between the terminal acetylene in **21**[23] and (*Z*)-3-iodobut-2-en-1-ol. Alcohol **22** was then converted to the phenyl sulfide **13** with 54% yield. The nitrogen-containing inhibitor **18** was synthesized by oxidation of allylic alcohol **22** with MnO_2, followed by imine formation using phenyl amine and then reduction to the amine.

2.2. In vitro assays and kinetic analyses

Recombinant AtNCED3 including a C-terminally located glutathione-S transferase fusion tag was expressed in *Escherichia coli* and purified by affinity chromatography. In vitro assays demonstrated the functionality of the recombinant purified enzyme product. Sample HPLC profiles (Supplementary data Fig. 1) show cleavage of the 9′-*cis*-neoxanthin **2** substrate (t_R 14.2 min. with three maxima at 415, 438 and 467 nm) producing the expected C_{25}-allenic apo-aldehyde cleavage product (t_R 11.6 min. with a maxima of 423 nm). Further kinetic analysis fitted by non-linear regression analysis defined a K_m of 24 μM (Fig. 4). This value correlates well with the K_m′s of 27 μM and 49.0 μM determined previously for VP14 and VuNCED1.[18,24]

Using this recombinant enzyme and assay system, the eight potential inhibitor compounds were tested for their relative ability to inhibit AtNCED3 activity at 1 mM concentration (Fig. 5). Compounds **12**, **17** and **18** completely inhibited AtNCED3 activity at 1 mM, while **13** inhibited AtNCED3 activity by 75%. Compound **12** is one of the stereoisomers of racemic **13**. The latter being easier to synthesize (and thus of higher potential practical application), it was decided to move forward with compounds **13**, **17** and **18** for detailed in vitro and in vitro testing. Dixon plots indicated that compounds **13**, **17** and **18** competitively inhibit recombinant AtNCED3 with K_i′s comparable or better than those observed for ABM and ABM-SG (Table 1 and Supplementary data Fig. 2).

2.3. Homology modeling and SLCCD inhibitor docking

Recently a crystal structure was determined for *Synechocystis* apocarotenoid-15,15′-oxygenase (ACO), a fungal homologue of the NCEDs.[25] AtNCED3 shares 25% identity and 45% similarity with ACO at the amino acid level. Homology modeling using the Swiss-Model servers generated a hypothetical protein structure of AtNCED3 which maintained the octahedral coordination of the four active site histidines at 2.14, 2.05, 2.16 and 2.31 Å from the iron atom for H164, H211, H276 and H450, respectively.[26] Structural differ-

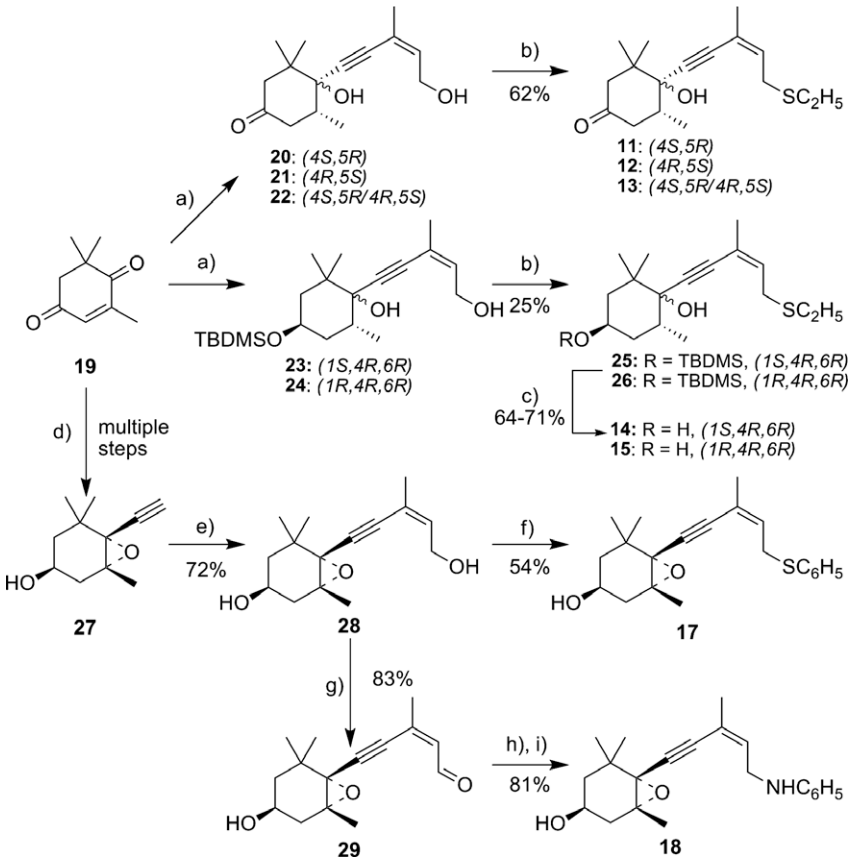

Figure 3. Synthesis of AtNCED3 SLCCD inhibitors. (a) See Ref. 20; (b) *n*-Bu_3P, $(C_2H_5S)_2$; (c) TBAF, THF; (d) see Ref. 22; (e) (*Z*)-3-iodobut-2-en-1-ol, $(Ph_3P)_4Pd$, CuI, $(i\text{-}Pr)_2NH$; (f) *n*-Bu_3P, $(C_6H_5S)_2$; (g) MnO_2; (h) $C_6H_5NH_2$, Δ; (i) $NaBH_4$.

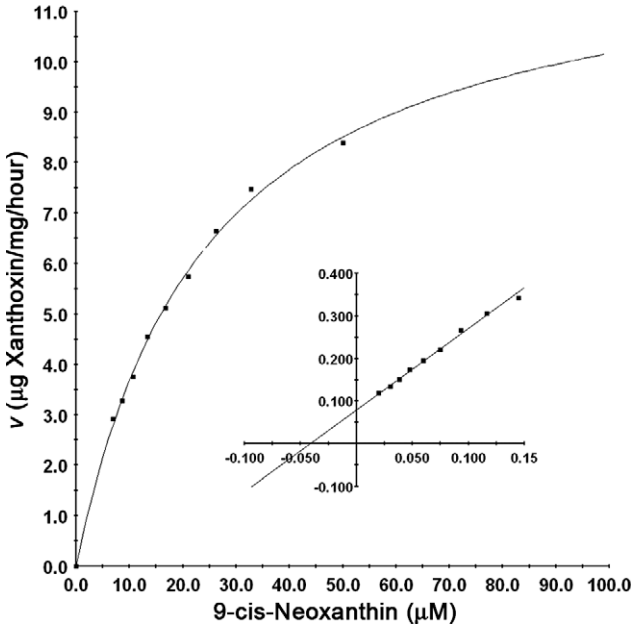

Figure 4. Kinetic analysis of recombinant purified AtNCED3 activity. Michaelis–Menton plot for cleavage of 9-*cis*-neoxanthin **2** by recombinant AtNCED3 indicating a K_m of 24 µM.

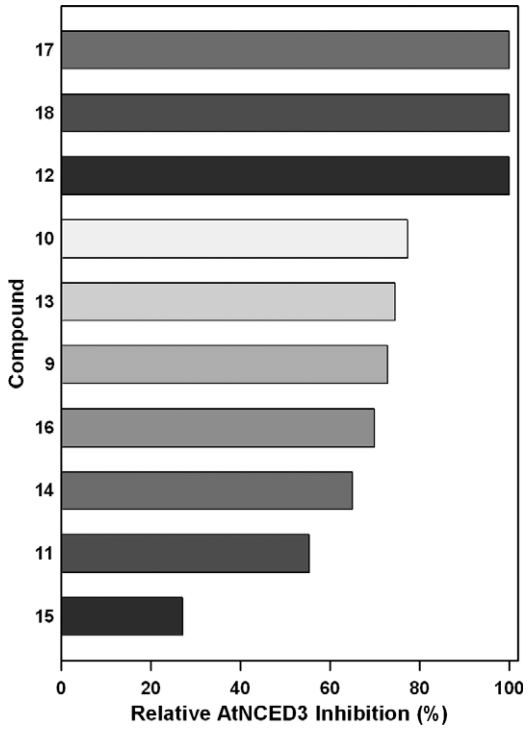

Figure 5. Relative inhibition of recombinant AtNCED3 activity by various SLCCD compounds at 1 mM concentration.

ences between the AtNCED3 model and ACO were limited to small surface exposed loops related to a few minor alignment gaps. As controls to test the AtNCED3 model, 9′-*cis*-neoxanthin **2**, the substrate of ACO (all-*trans*-(3R)-hydroxy-8′-apo-β-carotenol (3-ON)), and

Table 1
Kinetic parameters for AtNCED3 cleavage of the substrate 9-*cis*-neoxanthin **2,** and inhibitory effects of SLCCD inhibitor compounds

Compound	K_i (μM)	K_m (μM)
9-*cis*-Neoxanthin	–	24
13	93	–
17	57	–
18	87	–
10 (ABM-SG)	86	–
9 (ABM)	132	–

xanthoxin **4** structures were docked (Fig. 6A and Supplementary data Fig. 3A and B). The 3-ON molecule docked to the AtNCED3 model with a similar orientation as observed in the ACO crystal with its β-ionone ring oriented towards the tunnel entrance but shifted in toward the catalytic site by 5 Å. This positions the C12 and C13 bond within 3.95 Å of the iron atom and 2.10 Å of a coordinated active site water molecule. Docking of 9-*cis*-neoxanthin **2** resulted in the epoxide ring entering the protein channel first, yielding a final orientation with the C11–C12 bond 4.4 Å away from and directly over the iron atom and 2.3 Å away from the active site water molecule. The xanthoxin molecule docked in the opposite orientation from the 9-*cis*-neoxanthin substrate, with its epoxide ring towards the tunnel entrance and its C10 carbon atom 3.6 Å and 1.9 Å from the iron atom and water molecule, respectively.

Docking results correlated well with the in vitro enzyme assay data. Structures representing **12** (the more active stereoisomer of the racemic compound **13**), **17** and **18** (Fig. 6B and C and Supplementary data Fig. 3C, respectively) all docked in the same orientation as xanthoxin, in close proximity to the iron atom in the binding pocket. The nitrogen of **18** docked 2.67 Å away from the iron atom. The sulfur atoms of **12** and **17** docked 2.84 and 2.65 Å away from the iron atom, respectively. Other SLCCD inhibitor molecules that performed poorly in the in vitro trials generally were not targeted to the catalytic site of the binding pocket, or in some instances were not targeted to the binding pocket at all during docking.

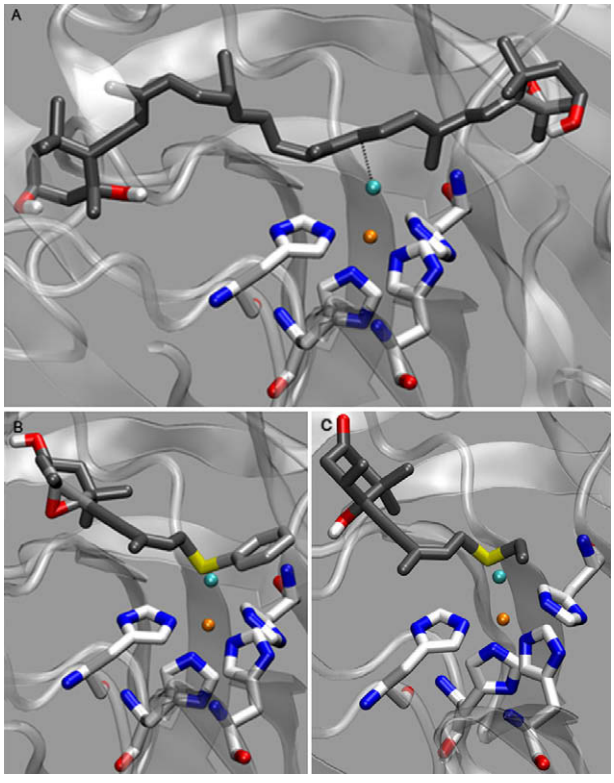

Figure 6. Computational docking of compounds to the AtNCED3 homology model. Docking was performed using the Autodock v3.1 software.[38] Conserved histidine residues are shown coordinating the iron (orange). The active site water (light blue) is shown in relation to the docked molecules. Molecules include (A) 9-*cis*-neoxanthin **2**, (B) compound **17** and (C) compound **12**. Sulfur heteroatoms in the two SLCCD compounds are highlighted in yellow.

2.4. Effect of SLCCD inhibitors on ABA accumulation under osmotic stress

A. thaliana plants were treated with either ABM **9** or the inhibitor compounds **13**, **17** and **18**, to evaluate their ability to reduce ABA biosynthesis induced by an osmotic stress. Essentially plants were treated ± inhibitor compound for 2 h followed by mannitol stress-treatment in the presence of the same compounds. Mannitol stress has been shown to result in loss of turgor with a corresponding increase in ABA levels through the induction of AtNCED3 in *A. thaliana*.[7,27] As expected, mannitol treatment alone resulted in an elevation of the levels of ABA and catabolites peaking 24 h after the imposition of treatment, compared to the levels in non-treated/non-stressed plants (Fig. 7). Accumulation of ABA and catabolites dropped off by 48 h as described previously.[28] Treatment with compound **13** for 2 h prior to and then during mannitol stress-treatment resulted in levels of ABA and catabolites remaining comparable to those of the non-treated/non-stressed control plants in the first 6 h. By 24 h, the total levels of ABA and catabolites in the compound **13** treated plants increased to only 8211 pmol/g, significantly below those of the mannitol-stressed only plants (15,147 pmol/g). Similar treatment of plants with ABM **9** resulted in higher levels of ABA and catabolites at the first time point, with levels remaining constant (and higher than those for treatment with compound **13**) over the remaining time course of the experiment. The remaining two inhibitors, **17** and **18**, were less effective than **13** in reducing the effect of the osmotic stress on ABA and catabolite pools. Interestingly, the overall effect observed for compound **13** is not represented in individual plots of ABA levels (or any one other catabolite) alone (Supplementary data Fig. 4). It is only when total accumulation of ABA and its catabolites are considered that the overall effect becomes evident.

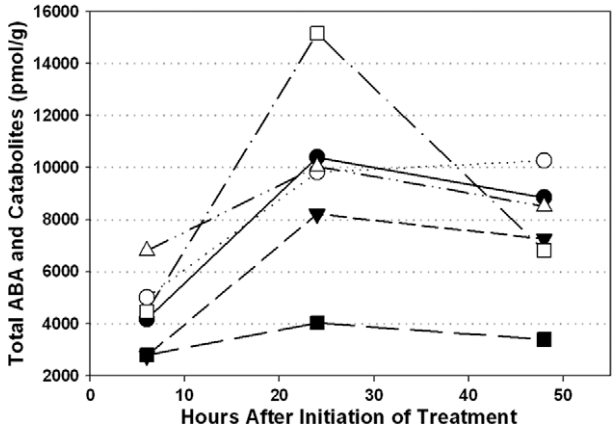

Figure 7. Total ABA metabolite levels in mannitol stressed *Arabidopsis thaliana* plants treated with SLCCD inhibitors. Plants were treated with 33 μM inhibitors (compounds **13** (inverted closed triangles), **17** (closed circles), **18** (open circles) and ABM **9** (open triangles)) for 2 h prior to being stressed with mannitol. Plants were harvested 6 h after the inhibitor treatment and compared to plants that were mannitol stressed only (open squares), or non-treated/non-stressed plants (closed squares). Metabolites quantified and summed at each time point include abscisic acid-glucose ester, dihydrophaseic acid, phaseic acid and abscisic acid.

2.5. Effect of SLCCD inhibitors on *A. thaliana* seed germination

Seed germination assays were performed for compounds **13**, **17** and **18** to assess the ABA-like character of the inhibitors.[29] Inhibitors had relatively little effect on seed germination at low concentration compared to non-inhibitor treated and ABA treated controls (Fig. 8). At increasing concentrations (0.33 μM) the inhibitors did lead to reductions of seed germination by approximately 15%, compared to 47% for the (+)-ABA **1**. Both compounds **13** and **17** reduced seed germination by 26% at 1 μM while **18** showed a more pronounced effect with a 50% reduction compared to 61% for (+)-ABA **1**. At the highest concentration tested, compound **13** still only had a modest impact on seed germination at 38% reduction, while compounds **17** and **18** showed 51% and 71% reductions, respectively, compared to 96% for (+)-ABA **1**.

2.6. Effect of SLCCD inhibitors on target gene transcript levels under osmotic stress

In light of the observed effectiveness of compound **13** in moderating ABA and catabolite levels in vitro and its limited effect on seed germination, it was targeted for further evaluation. Specifically, quantitative reverse-transcription PCR was used to assess inhibitor induced changes in gene transcript levels in mannitol stressed plants. The gene targets chosen for this purpose were *AtNCED3*, the ABA and drought inducible *Rd29B* and the ABA (inducible) catabolic genes *CYP707A1* and *CYP707A3*. Transcript levels were normalized against UBQ10 mRNA levels.[5,30,31] Mannitol treatment led to the induction of expression of all four target genes within 4 h of the stress-treatment (Fig. 9). Subsequently the mannitol-induced gene transcription levels decrease back to non-treated/non-stressed levels by 24 h post-treatment and remained low through 48 h (Supplementary data Figs. 5 and 6). In general, pre-treatment with compound **13** at both 10 and 33 μM concentrations prior to mannitol-stress led to reductions in the accumulation of mRNA transcript levels at 6 h post-compound treatment for *Rd29B*, *CYP707A1* and *CYP707A3* compared to the mannitol-stressed control (Fig. 9A). The inhibition of mannitol-induced *Rd29b* transcription by compound **13** (about 90%) is especially striking and is consistent with the mannitol effect on *Rd29b* being primarily mediated by ABA. This result indicates the potential of this inhibitor for dissecting the role of ABA in physiological and developmental processes. As observed in mannitol stressed only plants, transcript levels in compound **13** pre-treated plants decreased back to non-treated/non-stressed levels by 24 h and remained low through 48 h (Supplementary data Fig. 5). In addition to this, compound **13** was also found to decrease the relative expression levels of *AtNCED3* in mannitol stressed plants (Fig. 9B). While the former results emphasize the lack of ABA-like character for compound **13**, the moderation of *AtNCED3* transcription represents a useful inhibitor-dependent side-effect that likely further contributes to lowering ABA levels *in planta*. Testing of compounds **17** and **18** demonstrated similar, although not as pronounced effects on *AtNCED3* expression (Fig. 9B, Supplementary data Fig. 6).

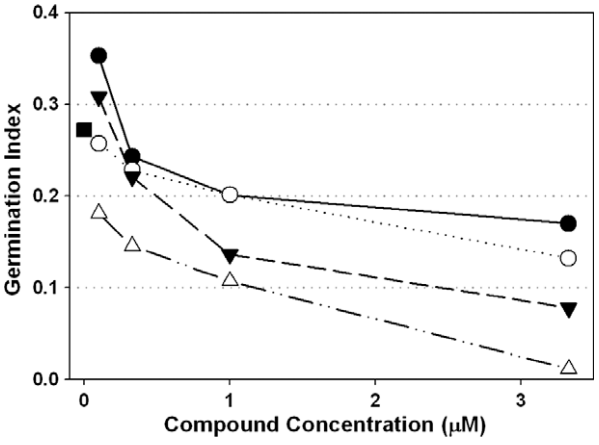

Figure 8. Germination of *Arabidopsis thaliana* plants in the presence of each of SLCCD inhibitor compounds **18** (inverted closed triangles), **13** (closed circles), **17** (open circles), (+)-ABA **1** (open triangles), and germination of plants on media without added compounds (closed square).

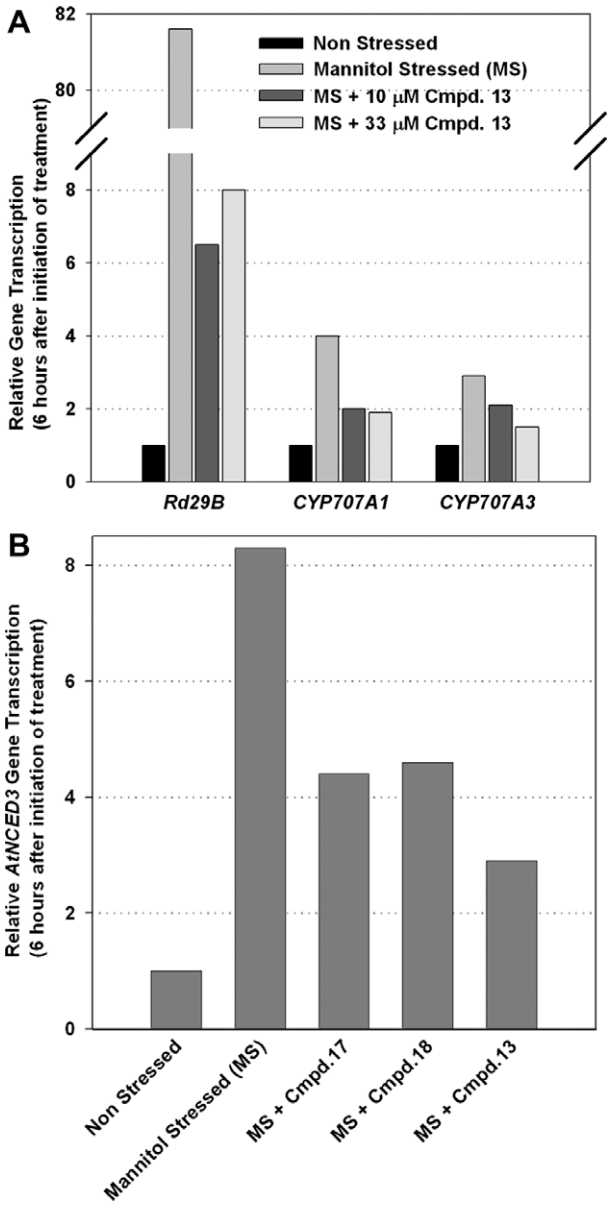

Figure 9. Target gene transcript levels in mannitol stressed *Arabidopsis thaliana* plants treated with SLCCD inhibitors. (A) Effect of compound **13**. Plants were treated with 10 or 33 μM compound **13** for 2 h prior to being stressed with mannitol. Plants were harvested 6 h after the SLCCD compound treatment and compared to mannitol stressed only plants or non-treated/non-stressed plants. Target genes included *Rd29B*, *CYP707A1* and *CYP707A3*. Transcript levels were normalized against the *UBQ10* gene. (B) Effects of SLCCD compounds on *AtNCED3* expression. Experiments were carried out as described for A, but with each of SLCCD compounds **13**, **17** and **18**.

3. Discussion

3.1. Design/synthesis and inhibitory activities of SLCCD inhibitors

The design of inhibitors described herein focuses on specific interaction with the non-heme iron atom within AtNCED3, a definitive motif of carotenoid cleavage enzymes. It was envisioned that a molecule maintaining characteristics of the native enzyme substrate 9-*cis*-neoxanthin **2** or xanthoxin **4** product, but presenting a nitrogen or sulfur heteroatom might specifically occupy the active site of the enzyme with the heteroatom interacting with the non-heme iron, resulting in inactivation of the enzyme. Similar concepts have been applied to inhibitors of other dioxygenase enzymes.[32,33]

In earlier ABA structure activity studies, analogs with the side chain having a triple bond conjugated to a *cis* double bond were found to be highly active and were also readily synthesized.[20] Therefore the enyne feature was incorporated into the design of the present set of eight potential ABA biosynthesis inhibitors. The epoxy alcohol analogs **17** and **18,** which most closely resemble the substrate and product of the NCED, strongly inhibited the NCED enzyme activity in vitro, and demonstrated higher inhibitory function than ABM **9** in this assay. However, in the experiment simulating drought stress, **17** and **18** were relatively weak inhibitors of ABA biosynthesis. As well, the aniline derivative **18** had a fairly pronounced (and undesirable) ABA-like effect on seed germination, with the thiophenyl analog **17** demonstrating a moderate effect. In addition, these compounds were prepared from the epoxy alkyne **25**, a compound that was not readily accessible, so these structural types were not pursued.

Compounds with a tertiary alcohol at the junction of ring and side chain and either ketone or alcohol at C-4 were also envisioned to be possible inhibitors, as the general shape of the molecule and oxygen atom would be maintained. The keto allylic alcohol precursors **20**–**22** were more conveniently prepared, affording both racemic and enantiomerically pure compounds. This was desirable as we had found earlier that the individual enantiomers **20** and **21** of the allylic alcohol **22** had different properties as competitive inhibitors of ABA perception.[34] The analog **20** competitively blocked ABA perception, while its enantiomer was a weak ABA agonist. On observing significant NCED inhibition with the racemic compound **13**, comparable with that of ABM **9** and ABM-SG **10**, we anticipated similar differences might be found in the present case, and the thioethyl derivatives of compounds **20** and **21** were synthesized and tested**.** Again, the stereochemistry of the analogs had an effect. Compound **12** inhibited the enzyme as strongly as the more xanthoxin-like compounds, while the other enantiomer **11** had reduced activity in the in vitro enzyme assay.

Two diasteromeric hydroxy compounds **14** and **15** were synthesized to explore the effect of changing the oxidation level of the C-4 or position of the oxygen atom. In the in vitro enzyme assay, the hydroxyl compounds did not afford greater activity, and were not pursued. Compound **16** was incorporated into the set of test molecules to determine if positioning the sulfur atom further from the cyclohexanone ring would have an effect on activity compared to that of **13**.

3.2. Computational analysis of SLCCD inhibitor-enzyme complexes

In the ACO structure the binding pocket entrance is proposed to act as a bottleneck, arresting movement of 3-ON to the interior and positioning the C15–C15′ bond over the iron molecule in a trans conformation.[25] In contrast, AtNCED3 must accept substrate molecules with rings at both extremities, and thus it would be expected that the binding pocket entrance be sufficiently large to allow ring structures to enter the cavity. Therefore in contrast to ACO, AtNCED3 likely determines substrate positioning based on where the molecule interacts with the internal terminus of the binding pocket. Docking to the AtNCED3 model highlights that this is likely the case, as 3-ON was oriented with its C13–C14 bond over the iron, and the β-ionone ring pulled inside the tunnel entrance. Docking of 9′-*cis*-neoxanthin **2** resulted in the epoxide ring being buried in the AtNCED3 catalytic pocket. This positioned the C11–C12 bond over the iron atom in a suitable position for catalytic cleavage at the expected location. These results emphasize the validity and potential utility of the AtNCED3 model.

The xanthoxin **4** molecule docked with its epoxide ring in the opposite orientation (similar to 3-ON) to that of the 9′-*cis*-neoxanthin **2**. While this likely does not represent its native orientation following cleavage of the 9-*cis*-neoxanthin **2** substrate, it emphasizes the accommodating size of the AtNCED3 entrance tunnel and that the preferred orientation of single ring containing molecules is with the ring pointing toward the entrance. Docking results for the SLCCD inhibitors seem to follow this preference with the hydroxylated rings preferentially pointing toward the entrance.

In the ACO crystal structure a coordinated water molecule occupies the fifth ligand position within the iron octahedral coordination structure. The water molecule, theorized to be an oxygen donor and required for catalytic activity, is located 3.2 Å from the C15 of the substrate and 2.07 Å from the non-heme iron atom.[25] Each of the three active SLCCD inhibitors docked with their heteroatoms (nitrogen or sulfur) within 2.8 Å of the iron atom such that they would be sufficient to occupy the coordinate space of the water molecule in the ACO structure and stop catalysis.

3.3. In vivo effects of SLCCD inhibitors

The basic premise of this work lies in the design of inhibitors that bind to and inactivate the NCED enzyme responsible for the first committed step in ABA **1** biosynthesis. In a recent study on effects of drought stress on signaling and gene expression in *Arabidopsis*, it had been shown that the levels of ABA and its catabolites phaseic acid **6**, dihydrophaseic acid **7** and ABA glucose ester **8** were all found to increase on imposition of the stress.[28] In the present study to compare the effects of potential inhibitors on ABA biosynthesis capacity, an osmotic stress treatment of *Arabidopsis* plants was substituted for the drought stress. ABA biosynthetic inhibitors were designed and tested and in the case of compound **13** were shown to significantly reduce the accumulation of ABA **1** and the catabolites **6**–**8** in plants subjected to osmotic stress. While the rationale for inhibitor design was based on maintaining structural characteristics similar to the enzymes substrate and products to maximize specificity, this also meant that the inhibitors share structural characteristics with ABA **1** itself. Obviously an inhibitor of ABA **1** biosynthesis should not mediate ABA signaling.

Toward assessing the ABA-like character of the inhibitors their ability to mediate known ABA **1** effects at the levels of seed germination and gene regulation were determined. In general, the SLCCD inhibitors were found to be weaker germination inhibitors than (+)-ABA **1**, with compound **13** having 60–70% less effect. Interestingly, low concentrations of compounds **13** and **17** had slight promotion effects on seed germination. As well, treatment of mannitol-stressed plants with compound **13** led to a reduction of transcript levels for three genes known to be (+)-ABA **1** inducible.[5,30] The reduction of transcription mediated by this inhibitor is in agreement with previous observations made for alternate inhibitors and likely results from the reduction of endogenous ABA **1** levels.[17] Overall, these results emphasize that SLCCD inhibitor **13** does not generally simulate ABA-inducible responses and thus does not maintain ABA-like characteristics.

Finally, these pilot in vitro studies demonstrate that mannitol stress leads to induction of *AtNCED3* gene expression as reported previously.[7] While stress-induced, it is not clear whether AtNCED3 is specifically ABA-inducible. But from the results reported here, it is clear that application of the SLCCD inhibitors significantly reduces *AtNCED3* mRNA levels under stress conditions, which would further contribute to reducing ABA **1** biosynthesis *in planta*. While this characteristic was not specifically sought in designing the inhibitors, in terms of the overall objective of inhibiting ABA **1** biosynthesis, a reduction in the primary biosynthetic enzyme is a very useful side-effect.

The relatively poor effects of inhibitors **17** and **18** *in planta* were surprising considering their effectiveness in vitro and docking results *in silico*. This lack of efficacy in vitro could be due to many factors, including stability of the different compounds in the plant and the presence of the hydrophobic aromatic rings in both **17** and **18** structures, possibly reducing their permeability through the roots and transport to the site of action. This lack of efficacy in moderating ABA levels in vitro could be due to many factors, including stability of the different compounds in the plant and the presence of the hydrophobic aromatic rings in both **17** and **18** structures, possibly reducing their permeability through the roots and transport to the site of action. The discrepancy between in vitro and in vitro results is consistent also in the *AtNCED3* expression profiling where **13** led to the highest reduction of stress-induced gene expression.

4. Conclusions

While in vitro studies identified SLCCD compound **17** as the most promising candidate inhibitor, hormone profiling data convincingly demonstrated that SLCCD **13**, a more easily synthesized racemic compound, best met the objective of reducing the total ABA metabolite levels *in planta*. Overall, these sesquiterpenoid-like inhibitors present new tools for controlling and investigating ABA biosynthesis, regulation and effects.

5. Experimental

5.1. Synthesis of ABA analogue inhibitors

5.1.1. (4*S*,5*R*)-(3′*Z*)-4-(5′-(Ethylthio)-3′-methylpent-3′-en-1′-ynyl)-4-hydroxy-3,3,5-trimethylcyclohexanone (11)

A solution of alcohol **20**[20] (25 mg, 0.1 mmol), ethyl disulfide (25 μL, 0.2 mmol) and *n*-Bu_3P (49 μL, 0.2 mmol) in CH_2Cl_2 (1.5 mL) was stirred at room temperature for 4.5 h. Ethanol (1 mL) was added to the reaction and the resulting mixture was stirred for 20 min. Ethanol was removed by evaporation and CH_2Cl_2 (15 mL) was added. The organic phase was washed with 0.5 N NaOH and brine successively, dried and concentrated to give a residue which was purified by FCC (ethyl acetate/hexane, 15:85 v/v) to provide **11** (19.2 mg, 62%) and recover **20** (4 mg, 19%). $[\alpha]_D^{25}$ −16 (*c* 0.48, $CHCl_3$); IR (KBr): 3463, 2975, 2872, 1688 cm^{-1}; ^1H NMR ($CDCl_3$) δ: 5.76 (1H, dt, 1.25, 7.75 Hz, =CH), 3.31 (2H, d, 8.75 Hz, CH_2S), 2.65 (1H, d, 14.25 Hz, H-2), 2.48 (2H, q, 7.5 Hz, SCH_2CH_3), 2.29 (3H, m, H-5 and H-6), 2.08 (1H, d, 14.25 Hz, H-2), 1.89 (3H, s, CH_3), 1.22 (3H, t, 7.5 Hz, SCH_2CH_3), 1.20 (3H, s, CH_3), 1.14 (3H, s, CH_3), 0.97 (3H, s, CH_3); ^{13}C NMR ($CDCl_3$) δ: 209.2, 134.2, 119.5, 92.6, 86.8, 77.4, 52.9, 47.0, 42.2, 37.4, 31.6, 25.9, 25.4, 23.2, 20.8, 16.6, 14.9; HRMS EI^+ *m/z* calcd for $C_{17}H_{26}O_2S$: 294.1654, found: 294.1655.

5.1.2. (4*R*,5*S*)-(3′*Z*)-4-(5′-(Ethylthio)-3′-methylpent-3′-en-1′-ynyl)-4-hydroxy-3,3,5-trimethylcyclohexanone (12)

A solution of alcohol **21**[20] (28 mg, 0.11 mmol), diethyl sulfide (28 μL, 0.22 mmol) and *n*-Bu_3P (55 μL, 0.22 mmol) in CH_2Cl_2 (2 mL) was stirred at room temperature for 6 h. Work up as described above, followed by purification by FCC (ethyl acetate/hexane, 15:85 v/v) to afford **12** (22 mg, 63%). $[\alpha]_D^{25}$ +15 (*c* 1.0, $CHCl_3$). The spectral characterization data was identical to enantiomer **11**.

5.1.3. (4*S*,5*R*/4*R*,5*S*)-(3′*Z*)-4-(5′-(Ethylthio)-3′-methylpent-3′-en-1′-ynyl)-4-hydroxy-3,3,5-trimethylcyclohexanone (13)

A solution of allylic alcohol **22**, protected as the neopentylglycol ketal[20], (34 mg, 0.1 mmol), ethyl disulfide (34 μL, 0.27 mmol) and *n*-Bu_3P (62 μL, 0.25 mmol) in CH_2Cl_2 was stirred at room temperature for 4.5 h. Work up as described above, followed by purification by FCC (ethyl acetate/hexane, 10:90 v/v) to afford the sulfide (22.1 mg, 58%). ^1H NMR ($CDCl_3$) δ: 5.67 (1H, ddq, 1.5, 7.75, 7.75 Hz, =CH), 3.54 (2H, d, 11.25 Hz, OCH_2), 3.36 (2H, ddd, 1.75, 11.25, 13.25 Hz, OCH_2), 3.31 (2H, dd, 0.75, 7.75 Hz, SCH_2), 2.48 (2H, q, 7.5 Hz, SCH_2CH_3), 2.24 (1H, dd, 3.25, 14.25 Hz, H-2), 2.18 (1H, m, H-5), 1.96 (1H, dt, 3.25, 13.5, H-6), 1.87 (3H, d, 1.0 Hz, CH_3), 1.57 (1H, dd, 13.5, 13.5 Hz, H-6), 1.46 (1H, d, 14.25 Hz, H-2), 1.22 (3H, t, 7.5 Hz, CH_3), 1.12 (3H, s, CH_3), 1.09 (3H, s, CH_3), 1.04 (3H, d, 7.5 Hz, CH_3), 1.04 (3H, s, CH_3), 0.82 (3H, s, CH_3). To a solution of the ketal protected sulfide (160 mg, 0.4 mmol) in acetone (5 mL) was added 2 N HCl (8 drops). The mixture was stirred at room temperature for 40 min. After evaporation of acetone, ether was added and washed with satd $NaHCO_3$, dried and concentrated to give a residue which was purified by FCC (ethyl acetate/hexane 20:80 v/v) to provide **13** (100 mg, 80%). The spectral characterization data was identical to pure enantiomer **11**.

5.1.4. (1*S*,4*R*,6*R*)-(3′*Z*)-1-(5′-(Ethylthio)-3′-methylpent-3′-en-1′-ynyl)-2,2,6-trimethylcyclohexane-1,4-diol (14)

A solution of allylic alcohols **23** and **24**[20] (200 mg, 0.55 mmol), $(C_2H_5S)_2$ (102 μL, 0.83 mmol) and *n*-Bu_3P (203 μL, 0.83 mmol) in CH_2Cl_2 (5 mL) was stirred at room temperature for 6 h. Work up as described above, followed by purification by FCC (ethyl acetate/hexane, 5:95 v/v) to provide **25** (41 mg, 17%), **26** (18.4 mg, 8%) and recovery of the unreacted starting material (70 mg, 35%). For **25**: ^1H NMR ($CDCl_3$) δ: 5.67 (1H, dt, 1.5, 7.75 Hz, =CH), 3.92 (1H, m, H-4), 3.32 (2H, dd, 0.75, 7.75 Hz, CH_2S), 2.49 (2H, q, 7.25 Hz, SCH_2CH_3), 2.32 (1H, m, H-6), 1.87 (3H, d, 1.0 Hz, CH_3), 1.76 (1H, br s, OH), 1.62 (1H, dd, 3.5, 14.25 Hz, H-3), 1.57 (2H, m, H-5), 1.49 (1H, d, 14.25 Hz, H-3), 1.23 (3H, t, 7.25 Hz, SCH_2CH_3), 1.20 (3H, s, CH_3), 1.06 (3H, s, CH_3), 1.04 (3H, d, 6.5 Hz, CH_3), 0.86 (9H, s, $SiCMe_3$), 0 (6H, s, $SiMe_2$). To a solution of **25** (41 mg, 0.1 mmol) in THF (1.5 mL) was added TBAF (1 M solution in THF, 0.5 mL, 0.5 mmol). The reaction mixture was stirred at room temperature for 1 day and diluted with ether. The mixture was washed with water (10 mL × 3), dried, concentrated and fractionated by FCC (10% ethyl acetate/hexane, 10:90 v/v increased to 35:65 v/v) to provide **14** (21.3 mg, 71%). $[\alpha]_D^{25}$ −13 (*c* 0.94, CH_2Cl_2); IR (KBr): 3332, 2976, 2879, 1450 cm^{-1}; ^1H NMR ($CDCl_3$) δ: 5.67 (1H, dt, 1.5, 7.75 Hz, =CH), 4.0 (1H, m, H-4), 3.30 (2H, dd, 1.0, 7.75 Hz, CH_2S), 2.47 (2H, q, 7.5 Hz, SC_2H_5), 2.32 (1H, m, H-6), 1.85 (3H, s, CH_3), 1.63 (4H, m, H-5 and H-3), 1.19 (3H, t, 7.5 Hz, SC_2H_5), 1.19, (3H, s, CH_3), 1.08 (3H, s, CH_3), 1.03 (3H, d, 6.5 Hz, CH_3); ^{13}C NMR ($CDCl_3$) δ: 133.2, 120.0, 94.1, 85.7, 79.1, 66.8, 44.5, 40.1, 38.8, 31.9, 31.6, 27.5, 25.2, 23.3, 23.1, 16.1, 14.9; HRMS CI^+ NH_3 *m/z* calcd for $C_{17}H_{32}NO_2S$: 314.2154, found: 314.2162.

5.1.5. (1*R*,4*R*,6*R*)-(3′*Z*)-1-(5′-(Ethylthio)-3′-methylpent-3′-en-1′-ynyl)-2,2,6-trimethylcyclohexane-1,4-diol (15)

To a solution of **26**[20] (18.4 mg, 0.045 mmol) in THF (1.2 mL) was added TBAF (1.0 M solution in THF, 0.13 mL, 0.13 mmol). The reaction was stirred at room temperature for 1 day. Work up as for **14** to provide product **15** (8.5 mg, 64%) and recovered starting material (4.5 mg, 24%). $[\alpha]_D^{25}$ +10 (*c* 0.25, CH_2Cl_2); IR (KBr): 3388, 2968, 2922, 1458 cm^{-1}; ^1H NMR ($CDCl_3$) δ: 5.71 (1H, dt, 1.5, 7.75 Hz,

=CH), 3.87 (1H, m, H-4), 3.33 (2H, dd, 1.0, 7.75 Hz, CH_2S), 2.51 (2H, q, 7.7 Hz, SC_2H_5), 2.00 (1H, m, H-6), 1.88 (3H, d, 1.5 Hz, CH_3), 1.67 (1H, ddd, 2.5, 4.5, 12.75 Hz, H-5), 1.57 (1H, dd, 11.5, 12.5 Hz, H-5), 1.35 (1H, dd, 12.5, 24.25 Hz, H-3), 1.23 (3H, t, 7.25 Hz, CH_3), 1.13 (3H, s, CH_3), 1.07 (3H, d, 6.5 Hz, CH_3), 1.02 (3H, s, CH_3); ^{13}C NMR ($CDCl_3$) δ: 133.4, 119.9, 93.9, 86.3, 78.3, 66.2, 46.8, 41.7, 39.9, 35.7, 31.6, 27.0, 25.3, 23.2, 20.8, 16.5, 14.9; HRMS EI$^+$ *m/z* calcd for $C_{17}H_{28}O_2S$: 296.1810, found: 296.1822.

5.1.6. (*1R,3S,6R)-(3′Z)*-6-(5′-Hydroxy-3′-methylpent-3′-en-1′-ynyl)-1,5,5-trimethyl-7-oxa-bicyclo[4.1.0]heptan-3-ol (28)

A mixture of compound **27**[20] (18 mg, 0.1 mmol), (*Z*)-3-iodobut-2-en-1-ol (30 mg, 0.15 mmol), CuI (15 mg, 0.08 mmol) and $(Ph_3P)_4Pd$ (23 mg, 0.02 mmol) in $(i\text{-}Pr)_2NH$ (0.3 mL) was stirred at room temperature for 17 h. Satd NH_4Cl solution was added to quench the reaction. The mixture was extracted with ether, dried, concentrated and fractioned by FCC (ethyl acetate/hexane, 60:40 v/v) to provide compound **28** (18.1 mg, 72%). $[\alpha]_D^{25}$ −8.0 (*c* 1.2, $CHCl_3$); IR (KBr): 3333, 2959, 2923 cm^{-1}; ^1H NMR ($CDCl_3$) δ: 5.85 (1H, ddq, 1.0, 6.75, 6.75 Hz, =CH), 4.26 (2H, d, 6.75 Hz, =$CHCH_2$), 3.79 (1H, m, H-3), 2.32 (1H, ddd, 1.75, 5, 14.25 Hz, H-2), 1.84 (3H, d, 1 Hz, CH_3), 1.74 (1H, br s, OH), 1.61 (1H, dd, 8.75, 14.25 Hz, H-2), 1.57 (1H, m, H-4), 1.47 (3H, s,CH_3), 1.22 (3H, s, CH_3), 1.19 (1H, dd, 10.5, 13.0 Hz, H-2), 1.08 (3H, s, CH_3); ^{13}C NMR (C_6D_6) δ: 137.8, 119.1, 92.4, 84.3, 66.6, 63.8, 63.6, 61.5, 45.7, 40.0, 34.4, 30.0, 26.2, 22.9, 22.0; HRMS CI$^+$ *m/z* calcd for $C_{15}H_{23}O_3$: 251.1647, found: 251.1646.

5.1.7. (*1R,3S,6R)-(3′Z)* -1,5,5-Trimethyl-6-(3′-methyl-5′-(phenylthio)-pent-3′-en-1′-ynyl)-7-oxa-bicyclo[4.1.0]heptan-3-ol (17)

A solution of alcohol **28** (56.6 mg, 0.23 mmol), phenyl disulfide (98.9 mg, 0.45 mmol) and *n*-Bu_3P (112 μL, 0.45 mmol) in dry CH_2Cl_2 (3 mL) was stirred at room temperature for 3 h. Ethanol (1 mL) was added to the reaction and stirred for 30 min. Ethanol was evaporated off and more CH_2Cl_2 added. The organic phase was washed with 0.5 N NaOH, followed by water and then dried, concentrated, and fractionated by FCC (ethyl acetate/hexane, 30:70 v/v) to give product **17** (42 mg, 54%). $[\alpha]_D^{25}$ −16 (*c* 0.84, $CHCl_3$); IR (KBr): 3438, 2961, 2924, 1583 cm^{-1}; ^1H NMR ($CDCl_3$) δ: 7.31 (2H, m, C_6H_5), 7.23 (2H, m, C_6H_5), 7.14 (1H, m, C_6H_5), 5.73 (1H, ddq, 1.0, 7.5, 7.5 Hz, =CH), 3.82 (1H, m, H-3), 3.71 (2H, dd, 0.75, 7.5 Hz, CH_2S), 2.34 (1H, ddd, 1.75, 5.0, 14.5 Hz, H-2), 1.81 (3H, d, 1.0 Hz, CH_3), 1.63 (1H, dd, 8.5, 14.5 Hz, H-2), 1.58 (1H, m, H-4), 1.47 (3H, s, CH_3), 1.23 (3H, s, CH_3), 1.21 (1H, m, H-4), 1.10 (3H, s, CH_3); ^{13}C NMR ($CDCl_3$) δ: 135.9, 132.9, 129.3, 128.9, 126.0, 120.7, 91.7, 84.2, 67.1, 63.8, 63.7, 45.8, 39.8, 34.4, 33.9, 29.9, 25.7, 22.9, 21.7; HRMS EI$^+$ *m/z* calcd for $C_{21}H_{26}O_2S$: 342.1654, found: 342.1659.

5.1.8. (*1′R,4′S,6′R)-(2Z)*-5-(4′-Hydroxy-2′,2′,6′-trimethyl-7′-oxa-bicyclo[4.1.0]heptan-1′-yl)-3-methylpent-2-en-4-ynal (29)

A mixture of alcohol **28** (89 mg, 0.36 mmol) and MnO_2 (774 mg, 8.9 mmol) in petroleum ether (10 mL) and ethyl acetate (5 mL) was stirred at room temperature for 4 h. The reaction mixture was filtered through a pad of Celite 545® and washed with ethyl acetate. The combined filtrates and washings were concentrated and purified by FCC (ethyl acetate/hexane, 30:70 v/v) to afford aldehyde **29** (73.3 mg, 83%). $[\alpha]_D^{25}$ −11 (*c* 3.0, $CHCl_3$); IR (KBr): 3456, 2918, 1601, 1593 cm^{-1}; ^1H NMR (C_6D_6) δ: 10.27 (1H, d, 8.0 Hz, CHO), 5.88 1H, dd, 0.75, 8.0 Hz, =CH), 3.55 (1H, m, H-4), 2.03 (1H, ddd, 1.0, 5.0, 15.5 Hz, H-5), 1.46 (3H, d, 0.75 Hz CH_3), 1.36 (2H, m, H-3 and H-5), 1.27 (3H, s, CH_3), 1.13 (3H, s, CH_3), 1.11 (3H, s, CH_3), 0.99 (1H, dd, 10.0, 13.0 Hz, H-3); ^{13}C NMR (C_6D_6) δ: 190.8, 140.1, 136.3, 98.4, 82.5, 67.0, 63.4, 45.4, 39.8, 34.3, 29.6, 26.1, 24.1, 21.8; HRMS CI$^+$ *m/z* calcd for $C_{15}H_{21}O_3$: 249.1491, found: 249.1489.

5.1.9. (*1R,3S,6R)-(3′Z)*-1,5,5-Trimethyl-6-(3′-methyl-5′-(phenylamino)-pent-3′-en-1′-ynyl)-7-oxabicyclo[4.1.0]heptan-3-ol (18)

A solution of aldehyde **29** (16 mg, 0.065 mmol) and aniline (10 μL, 0.11 mmol) in ethanol (1.5 mL) was refluxed for 30 min. The reaction mixture was cooled to room temperature and then $NaBH_4$ (7.4 mg, 0.2 mmol) was added. The resulting mixture was stirred at room temperature for 15 min and water (3 mL) with glacial acetic acid (1 drop) was added. The ethanol was evaporated off and water phase was extracted with ether, dried, concentrated and fractionated by FCC (ethyl acetate/hexane, 35:65 v/v) to provide product **18** (17 mg, 81%). $[\alpha]_D^{25}$ −13 (*c* 1.4, $CHCl_3$); IR (KBr): 3410, 2960, 1602, 1504 cm^{-1}; ^1H NMR (C_6D_6) δ: 7.15 (2H, m, C_6H_5), 6.73 (1H, dd, 7.25, 7.25 Hz, C_6H_5), 6.52 (2H, dd, 1.0, 8.5 Hz, C_6H_5), 5.47 (1H, ddq, 1.5, 6.5, 6.5 Hz, =CH), 3.80 (2H, m, CH_2NH), 3.62 (1H, m, H-3), 2.09 (1H, ddd, 1.5, 5.0, 14.5 Hz, H-2), 1.67 (3H, d, 1.25, CH_3), 1.44 (3H, s, CH_3), 1.40 (2H, m, H-2 and H-4), 1.31 (3H, s, CH_3), 1.23 (3H, s, CH_3), 1.05 (1H, dd, 9.75, 13.0 Hz, H-4); ^{13}C NMR (C_6D_6) δ: 148.4, 136.5 129.5, 119.8, 117.7, 113.2, 92.9, 84.5, 66.6, 63.6, 45.7, 44.1, 40.0, 34.4, 30.1, 26.2, 22.9, 22.0; HRMS TOF$^+$ *m/z* calcd for $C_{21}H_{28}NO_2$: 326.2114, found: 326.2123.

5.1.10. (*2Z,4E)*-5-(1′-Hydroxy-2′,2′,6′-trimethyl-4′-oxocyclohexyl)-3-methylpenta-2,4-dienyl 2-(thiophen-2′′-yl) acetate (16)

To a solution of the allylic alcohol, racemic **20** from Ref. 20, (34 mg, 0.1 mmol), Et_3N (42 μL, 0.3 mmol) in CH_2Cl_2 (1.5 mL) was added 2-thiopheneacetyl chloride (18 μL, 0.15 mmol). The reaction mixture was stirred at room temperature for 4 h and diluted with CH_2Cl_2. The organic phase was washed with satd $NaHCO_3$, dried, concentrated and fractionated by PTLC (ethyl acetate/hexane, 20:80 v/v) to the ketal protected thiophene ester (13 mg, 28%). ^1H NMR ($CDCl_3$) δ: 7.19 (1H, d, 1.25 Hz, SCH), 6.93 (2H, m, thiophene CH=CH), 6.67 (1H, d, 15.5 Hz, CH=CH), 5.98 (1H, d, 15.5 Hz, CH=CH), 5.47 (1H, t, 7.0 Hz, =$CHCH_2O$), 4.80 (2H, d, 7.0 Hz, CH_2O), 3.82 (2H, s, $COCH_2$), 3.58 (2H, dd, 5, 10.25 Hz, OCH_2), 3.41 (2H, dd, 5, 10.25 Hz, OCH_2), 2.30 (1H, dd, 2.75, 14.5 Hz, H-3), 2.17 (1H, m, H-6′), 1.98 (1H, dd, 3.25, 14.25 Hz, H-5′), 1.86 (3H, s, CH_3), 1.40 (1H, d, 14.0 Hz, H-3′), 1.35 (1H, d, 14.0 Hz, H-3′), 1.12 (3H, s, CH_3), 1.06 (3H, s, CH_3), 0.85 (3H, s, CH_3), 0.78 (3H, s, CH_3), 0.77 (3H, d, 8.0 Hz, CH_3). To a solution of the ketal protected thiophene ester (13 mg, 0.028 mmol) in acetone (1.5 mL) was added 2 N HCl (2 drops). The mixture was stirred at room temp. for 1 h. After removing acetone, ether was added and washed with satd $NaHCO_3$, dried and concentrated to give a residue which was purified by FCC (ethyl acetate/hexane, 20:80 v/v) to provide **16** (8 mg, 75%). IR (KBr): 3517, 2959, 1714 cm^{-1}; ^1H NMR ($CDCl_3$) δ: 7.19 (1H, d, 1.5 Hz, SCH), 6.93 (2H, m, thiophene CH=CH), 6.80 (1H, d, 15.5 Hz, CH=CH), 6.12 (1H, d, 15.5 Hz, CH=CH), 5.54 (1H, t, 7.0 Hz, =$CHCH_2O$), 4.81(2H, d, 7.0 Hz, CH_2O), 3.82 (2H, s, $COCH_2$), 2.46 (1H, d, 15.0 Hz, H-3′), 2.30 (2H, m, H-5′ and H-6′) 2.13 (2H, m, H-5′ and H-3′), 1.90 (3H, s, CH_3), 1.02 (3H, s, CH_3), 0.90 (3H, s, CH_3), 0.85 (3H, d, 6.5 Hz, CH_3); ^{13}C NMR (C_6D_6) δ: 209.3, 170.4, 136.7, 135.6, 135.0, 129.9, 128.2, 126.8, 125.1, 123.1, 78.1, 61.0, 52.9, 47.1, 41.6, 37.4, 35.4, 25.2, 22.8, 20.9, 15.9; HRMS EI$^+$ *m/z* calcd for $C_{21}H_{28}O_4S$: 376.1708, found: 376.1720.

5.2. AtNCED In vitro assay substrate preparation

Fresh spinach was macerated under liquid nitrogen and extracted five times with three volumes of methanol/0.1% KOH. Samples were dried using a roto-evaporator, resuspended in acetone and then chilled on ice for 1 h. The solvent was subsequently transferred to a new flask, roto-evaporated and resuspended in acetonitrile/acetone (1:1) mixture. The mixture was applied to a gravity

flow column containing C-18 silica gel (Sigma) equilibrated in 65% acetonitrile/35% water (solvent C). The column was washed with 49% acetone (solvent D)/51% solvent A and 20 mL of 55% solvent D/45% solvent A while collecting 5 mL fractions. Fractions containing neoxanthin were pooled, dried, and resuspended in 100 μL of methanol. The pooled mixture was separated using an Agilent 1100 series HPLC and a Supelcosil LC-18 (25 cm × 10 mm, 5 μm) (Supelco) column equilibrated with solvent A. The HPLC method consisted of a linear gradient over 30 min from 100% solvent A to 100% solvent D with a flow rate of 4 mL/min at 22 °C and monitored with a PDA detector at 436 nm. The neoxanthin fractions were collected, dried and resuspended in ethanol. Neoxanthin was quantified by determining its OD439 using a PerkinElmer Lambda 35 UV–vis spectrometer and applying its extinction coefficient of 2243 (A1%1 cm).[30]

5.3. Recombinant AtNCED3 expression, purification and in vitro assays

AtNCED3 was over-expressed using the pRL296 expression vector (a gift from M. Cygler, BRI, Montreal) in *E. coli* (BL21)DE3 cells as a glutathione-*S*-transferase fusion protein and affinity purified using glutathione sepharose 4 fast flow resin (GE Healthcare) as described previously.[35] Essentially, cells were grown to an OD600 of 0.45 at 37 °C and 200 rpm shaking. The culture was induced with 1 mM isopropyl-β-D-thiogalactoside for 16 h at 15 °C and 200 rpm shaking. The cells were pelleted and resuspended in 50 mM Tris–HCl (pH 8.0) 1 mM DTT and 0.5% protease inhibitor cocktail set III (CalBiochem). Cells were lysed using a french press at 20,000 psi and affinity purified as per manufacturer's instructions (GE Healthcare). Protein concentration was determined by the method of Bradford.[36]

Enzymatic assays contained 100 mM bis–tris (pH 6.7), 5 μM $FeSO_4$, 10 mM ascorbate, 0.05% Triton X-100, catalase (1 mg/mL), neoxanthin and inhibitor to a total volume of 5 μL of ethanol and 8 μg AtNCED3 to a total assay volume of 100 μL. Assays were incubated at 22 °C for 20 min. The assays were stopped with the addition of 50 μL of 25% Triton X-100 and extracted with 150 μL of ethyl acetate. All procedures were performed under red-light to minimize photo-induced damage to assay components and products.[6] Fine chemicals and solvents were purchased from Sigma–Aldrich. 75 μL of the assay extract was injected into an Agilent 1100 series HPLC machine equipped with a Supelcosil LC-18 (3.3 cm × 4.6 mm, 3 μm) (Supelco) column pre-equilibrated with 15% acetonitrile (solvent B)/85% water (solvent A). Solvent B increased to 35% over 10 min, followed by a linear gradient of 65% solvent B to 100% solvent D over 10 min. Solvent D was maintained at 100% for 2 min and then the column was returned to 15% solvent B for 5 min. The flow rate was maintained at 1.5 mL/min. and monitored with a photodiode array (PDA) detector at 436 and 262 nm.

Preliminary in vitro screening experiments of all selected potential inhibitors were not reproduced due to limitations in the availability of some of the compounds. Instead the top three performing inhibitors were selected for subsequent kinetic evaluation. Evaluation of recombinant AtNCED3 kinetic parameters for K_m was accomplished using Michaelis–Menten equation plotted with EnzFitter v2.0.18.0 (Biosoft). The K_i for inhibitors was determined using a Dixon plot and concentration ranges of 250, 200, 150, 100, 50 and 0 μM inhibitor in the presence of either 55, 30 or 10 μM 9-*cis*-neoxanthin **2**.[5]

5.4. Homology modeling of AtNCED3

A homology model of AtNCED3 was built using the X-ray crystal structure of *Synechocystis* sp. PCC 6803 ACO (pdb code: 2biw; available at the RCSB Protein Data Bank) at 2.39 Å resolution as a structural template.[25] To model AtNCED3, amino acid alignments were made between ACO, AtNCED3 and VP14. AtNCED3 shares 25% and 45% amino acid identity and similarity with ACO, and 64% and 76%, respectively with VP14.[37] Highly conserved amino acids including H183, H238, H304 and H484 forming the octahedral coordination of the non-heme iron required for catalysis of the dioxygenase reaction were used to aid in development of a suitable alignment and ultimately build the homology model. Homology modeling jobs were submitted to the Swiss-Model servers using the DEEPVIEW program as an interface.[26] Each generation of the AtNCED3 homology model was energy minimized within DEEPVIEW using 1000 steps of steepest descent followed by 1000 steps of conjugate gradient minimization until the RMS gradient of the potential energy was less than 0.01 kJ.

5.5. *In silico* docking of AtNCED3 active site SLCCD inhibitor interactions

Inhibitor structures were created using CS ChemOffice v9 (CambridgeSoft). *In silico* docking of inhibitor structures to the AtNCED3 homology model were performed using AutoDock v3.1 on a Silicon Graphics Octane2 Workstation.[38] Inhibitor structures were docked within a grid box encompassing the entire catalytic pocket of AtNCED3 corresponding to 80 × 36 × 30 points using a spacing of 0.375 Å between grid points. The docking parameters consisted of 20 Lamarckian Genetic Algorithm runs using a population size of 100 individuals and 1,000,000 energy evaluations. Final docked structures having orientations less than or equal to 0.5 Å root mean square deviation were clustered.

5.6. In vivo application of SLCCD inhibitors to *A. thaliana* Col-0

For each condition to be tested, three hundred wild-type *A. thaliana* Col-0 seeds (LEHLE) were sterilized, stratified and sewn onto 200 mL of Sunshine Mix #3 (Sun Gro) potting material in an 8 × 8 × 4 cm pot. Plants were watered continuously with 25 g/100 mL of 20–20–20 (PlantProd) fertilizer and grown at 22 °C with a 16 h photoperiod for 22 days. Plants were pre-treated with 50 mL/pot of Buffer A (10 mM HEPES pH 6.5) (Sigma) ± 10 or 33 μM test compound for 2 h. Plants were then soaked with 50 mL/pot of Buffer A containing 0.4 M mannitol (Sigma) ± 10 or 33 μM test compound. Non-treated/non-stressed control plants were simply soaked in Buffer A at the designated time points. Aerial plant tissue was harvested after 6, 12 and 48 h from the time of initial inhibitor treatment and flash frozen in liquid nitrogen. Half of the tissue samples were lyophilized for metabolite profiling and the other half taken for quantitative reverse-transcription polymerase chain reaction (qRT-PCR) analysis. While analytical experiments were carried out on pooled samples (~300 plants/condition), experiments were not replicated due to limitations in the availability of inhibitor compounds for treatments at high concentrations.

5.7. Metabolite profiling of *A. thaliana* hormone levels

Freeze-dried tissue was homogenized using a multi-tube ball mill (Mini-BeadBeater-96, Biospec Products Inc., Bartlesville, Oklahoma, USA) and 50 mg of each sample was weighed out into individual Falcon tubes. To each sample, 100 μL of a cocktail of internal standards comprised of (−)-5,8′,8′,8′-d4-ABA, (−)-7′,7′,7′-d3-PA, (−)-5,8′,8′,8′-d4-7′OH ABA, (−)-7′,7′,7′-d3-DPA and (+)-4,5,8′,8′,8′-d5-ABAGE, each at a concentration of 0.2 ng/μL and dissolved in a mixture of water/acetonitrile (1:1, v/v) with 0.5% glacial acetic acid, was added. Further, 3 mL of isopropanol/water/glacial acetic acid (80:19:1, v/v/v) extraction solvent was added, and samples were placed in the fridge (4 °C, in the dark) on an orbital shaker

at ~350 rpm. After 18–24 h, the samples were centrifuged at 4.4 krpm for 10 min, the supernatant was transferred to a disposable culture tube, and a second portion of 500 μL extraction solvent mixture was added to wash the pellet. After vortexing and centrifuging again at 4.4 krpm for 10 min, each wash was combined with its appropriate supernatant. The organic extract was dried under reduced pressure, then re-dissolved in 100 μL methanol/glacial acetic acid (99:1, v/v) followed by 900 μL of aqueous 1% glacial acetic acid. This mixture was extracted with 2 mL hexane, and then the aqueous layer was dried down under reduced pressure. The sample was further reconstituted in 2 mL aqueous 1% glacial acetic acid and loaded onto an Oasis MCX SPE cartridge (3 cc, Waters Corporation, Mississauga, Ontario, Canada). After a wash with 3 mL aqueous 1% glacial acetic acid, samples were eluted with 1 mL methanol/glacial acetic acid (99:1, v/v) and then dried down under reduced pressure. The extract was re-dissolved in 100 μL methanol/glacial acetic acid (99:1, v/v) followed by 900 μL of aqueous 1% glacial acetic acid. This mixture was further cleaned on an Oasis HLB SPE cartridge (1 cc, Waters Corporation, Mississauga, Ontario, Canada). After a wash with 1 mL aqueous 1% glacial acetic acid, the fraction containing ABA and ABA metabolites was eluted with 1 mL acetonitrile/water/glacial acetic acid (30:69:1, v/v/v) and then was evaporated to dryness. The final residue was dissolved in 200 μL of acetonitrile/water (15:85, v/v) containing 0.1% glacial acetic acid and 100 pg/μL (±)-3′,5′,5′,7′,7′,7′-d6-ABA as a recovery standard. Finally, the sample was subjected to LC–ES–MS/MS analysis and quantification, as described in Owen and Abrams, 2008.[39]

5.8. Seed germination assay

A. thaliana Col-0 seeds were sterilized by washing them with 10% sodium hypochlorite and 20% sodium dodecyl sulfate (Sigma) for 5 min and then rinsing four times with sterile water. Seeds were moist chilled for 4 days and then plated on germination medium (0.41% MS salts, 1% sucrose, 0.05% MES and 0.1% Gamborg's vitamins, pH 5.7, 0.7% agar) (Sigma) containing either 0.1, 0.33, 1.0 or 3.33 μM of inhibitor or (+)-ABA **1**. As a control, seeds were sewn and germinated on media only without inhibitors or (+)-ABA **1**. Germination was recorded over seven days and indexes calculated as described previously.[40] Experiments were not replicated due to limitations in the availability of inhibitor compounds for treatments at high concentrations.

5.9. Quantitative reverse-transcription PCR (qRT-PCR)

Frozen plant material (250 mg) was ground under liquid nitrogen and extracted for mRNA as suggested by the manufacturer (PolyA-Tract System 1000, Promega). The resulting mRNA was quantified and checked for quality using a Nano-Drop ND-1000 Spectrophotometer. QuantiTect Reverse Transcription Kit (Qiagen) was used to produce cDNA as directed by the manufacturer from 20 ng of starting mRNA. Quantitative PCR was performed on 1 μL of cDNA product using a Bio-Rad iCycler and the QuantiTect SYBR Green PCR Kit (Qiagen) coupled with QuantiTect Primer Assays (Qiagen) for the gene targets; AtNCED3 (NM_112304), Rd29B (NM_124609), CYP707A1 (NM_118043), CYP707A3 (NM_123902) and UBQ10 (NM_178968). The pre-validated primer sets are as follows indicated by the GeneGlobe (https://www1.qiagen.com/GeneGlobe/default.aspx) product name and (catalogue number): At_NCED3_1_SG (QT00769573), At_RD29B_1_SG (QT00840399), At_CYP707A1_1_SG (QT00808339), At_CYP707A3_1_SG (QT00739242), At_UBQ10_va.1_SG (QT01123745). Relative changes in transcript level were normalized using UBQ10 and quantified as previously described.[41]

Acknowledgments

This work was supported by the National Research Council of Canada. We would like to thank Tadao Asami for generously supplying us with quantities of ABM and ABM-SG used as controls in our study. This manuscript represents NRCC# 50133.

Supplementary data

Supplementary data associated with this article can be found, in the online version, at doi:10.1016/j.bmc.2009.01.076.

References and notes

1. Zeevaart, J. A.; Creelman, R. A. *Annu. Rev. Plant Physiol. Plant Mol. Biol.* **1988**, *39*, 439.
2. McCarty, D. R. *Annu. Rev. Plant Physiol. Plant Mol. Biol.* **1995**, *46*, 71.
3. Nambara, E.; Marion-Poll, A. *Annu. Rev. Plant Biol.* **2005**, *56*, 165.
4. Milborrow, B. V. *J. Exp. Bot.* **2001**, *52*, 1145.
5. Kushiro, T.; Okamoto, M.; Nakabayashi, K.; Yamagishi, K.; Kitamura, S.; Asami, T.; Hirai, N.; Koshiba, T.; Kamiya, Y.; Nambara, E. *EMBO J.* **2004**, *23*, 1647.
6. Schwartz, S. H.; Tan, B. C.; Gage, D. A.; Zeevaart, J. A. D.; McCarty, D. R. *Science* **1997**, *276*, 1872.
7. Iuchi, S.; Kobayashi, M.; Taji, T.; Naramoto, M.; Seki, M.; Kato, T.; Tabata, S.; Kakubari, Y.; Yamaguchi-Shinozaki, K.; Shinozaki, K. *Plant J.* **2001**, *27*, 325.
8. Qin, X.; Zeevaart, J. A. D. *PNAS* **1999**, *96*, 15354.
9. Burbidge, A.; Grieve, T. M.; Jackson, A.; Thompson, A.; McCarty, D. R.; Taylor, I. B. *Plant J.* **1999**, *17*, 427.
10. Chernys, J. T.; Zeevaart, J. A. D. *Plant Physiol.* **2000**, *124*, 343.
11. Iuchi, S.; Kobayashi, M.; Yamaguchi-Shinozaki, K.; Shinozaki, K. *Plant Physiol.* **2000**, *123*, 553.
12. Tan, B.-C.; Joseph, L. M.; Deng, W.-T.; Liu, L.; Li, Q.-B.; Cline, K.; McCarty, D. R. *Plant J.* **2003**, *35*, 44.
13. Endo, A.; Sawada, Y.; Takahashi, H.; Okamoto, M.; Ikegami, K.; Koiwai, H.; Seo, M.; Toyomasu, T.; Mitsuhashi, W.; Shinozaki, K.; Nakazono, M.; Kamiya, Y.; Koshiba, T.; Nambara, E. *Plant Physiol.* **2008**, *12*. pp. 108.116632.
14. Nagamune, K.; Hicks, L. M.; Fux, B.; Brossier, F.; Chini, E. N.; Sibley, L. D. *Nature* **2008**, *451*, 207.
15. Toh, S.; Imamura, A.; Watanabe, A.; Nakabayashi, K.; Okamoto, M.; Jikumaru, Y.; Hanada, A.; Aso, Y.; Ishiyama, K.; Tamura, N.; Iuchi, S.; Kobayashi, M.; Yamaguchi, S.; Kamiya, Y.; Nambara, E.; Kawakami, N. *Plant Physiol.* **2008**, *146*, 1368.
16. Creelman, R. A.; Bell, E.; Mullet, J. E. *Plant Physiol.* **1992**, *99*, 1258.
17. Kitahata, N.; Han, S.-Y.; Noji, N.; Saito, T.; Kobayashi, M.; Nakano, T.; Kuchitsu, K.; Shinozaki, K.; Yoshida, S.; Matsumoto, S. *Bioorg. Med. Chem.* **2006**, *14*, 5555.
18. Han, S.-Y.; Kitahata, N.; Sekimata, K.; Saito, T.; Kobayashi, M.; Nakashima, K.; Yamaguchi-Shinozaki, K.; Shinozaki, K.; Yoshida, S.; Asami, T. *Plant Physiol.* **2004**, *135*, 1574.
19. Baumeler, A.; Brade, W.; Haag, A.; Eugster, C. H. *Helv. Chim. Acta* **1990**, *73*, 700.
20. Lamb, N.; Abrams, S. R. *Can. J. Chem.* **1990**, *68*, 1151.
21. Isler, O.; Lindlar, H.; Montavon, M.; Rüegg, R.; Saucy, G.; Zeller, P. *Helv. Chim. Acta* **1956**, *39*, 2041.
22. Nakagawa, I.; Hata, T. *Tetrahedron Lett.* **1975**, *17*, 1409.
23. Furuichi, N.; Hara, H.; Osaki, T.; Mori, H.; Katsumura, S. *Angew. Chem., Int. Ed.* **2002**, *41*, 1023.
24. Schwartz, S. H.; Tan, B. C.; McCarty, D. R.; Welch, W.; Zeevaart, J. A. D. *Biochim. Biophys. Acta (BBA)—General Subj.* **2003**, *1619*, 9.
25. Kloer, D. P.; Ruch, S.; Al-Babili, S.; Beyer, P.; Schulz, G. E. *Science* **2005**, *308*, 267.
26. Schwede, T.; Kopp, J.; Guex, N.; Peitsch, M. C. *Nucleic Acids Res.* **2003**, *31*, 3381.
27. Creelman, R. A.; Zeevaart, J. A. D. *Plant Physiol.* **1985**, *77*, 25.
28. Huang, D.; Wu, W.; Abrams, S. R.; Cutler, A. J. *J. Exp. Bot.* **2008**, *59*, 2991.
29. Cutler, A. J.; Rose, P. A.; Squires, T. M.; Loewen, M. K.; Shaw, A. C.; Quail, J. W.; Krochko, J. E.; Abrams, S. R. *Biochemistry* **2000**, *39*, 13614.
30. Yamaguchi-Shinozaki, K.; Shinozaki, K. *Plant Physiol.* **1993**, *101*, 1119.
31. Norris, S. R.; Meyer, S. E.; Callis, J. *Plant Mol. Biol.* **1993**, *21*, 895.
32. Han, S.-y.; Inoue, H.; Terada, T.; Kamoda, S.; Saburi, Y.; Sekimata, K.; Saito, T.; Kobayashi, M.; Shinozaki, K.; Yoshida, S.; Asami, T. *Bioorg. Med. Chem. Lett.* **2002**, *12*, 1139.
33. Abe, M.; Matsuki, H.; Domae, M.; Kuwata, H.; Kudo, I.; Nakanishi, Y.; Hara, N.; Mitsuyama, T.; Furukawa, T. *Am. J. Respir. Cell Mol. Biol.* **1996**, *15*, 565.
34. Wilen, R. W.; Hays, D. B.; Mandel, R. M.; Abrams, S. R.; Moloney, M. M. *Plant Physiol.* **1993**, *101*, 469.
35. Guo, S.; Boyd, J.; Sammynaiken, R.; Loewen, M. C. *Biochemistry and Cell Biology* **2008**, *86*, 262.
36. Bradford, M. M. *Anal. Biochem.* **1976**, *72*, 248.
37. Nicolas Guex, M. C. P. *Electrophoresis* **1997**, *18*, 2714.
38. Morris, G. M.; Goodsell, D. S.; Halliday, R. S.; Huey, R.; Hart, W. E.; Belew, R. K.; Olson, A. J. *J. Comput. Chem.* **1998**, *19*, 1639.
39. Owen, S. J.; Abrams, S. R. In *Plant Hormones: Methods and Protocols*, 2nd Ed., Cutler, S., Bonetta, D., Eds.; Humana Press, A Part of Springer Science + Business Media, **2009**, pp. 39–51.
40. Walker-Simmons, M. K. *Plant, Cell Environ.* **1988**, *11*, 769.
41. Livak, K. J.; Schmittgen, T. D. *Methods* **2001**, *25*, 402.